

# Derivation of Far-field Gain Using a Gain Reduction Effect in the Fresnel Region

Ilkyu Kim<sup>1</sup>, Sun-Gyu Lee<sup>2</sup>, and Jeong-Hae Lee<sup>2</sup>

<sup>1</sup>C4I Team

Defense Agency for Technology and Quality, Daejeon, 35409, Republic of Korea  
ilkyukim@gmail.com

<sup>2</sup>Department of Electronics and Electrical Engineering  
Hongik University, Seoul, 04066, Republic of Korea  
gyul0206@gmail.com, jeonglee@hongik.ac.kr

**Abstract** — A handy method of calculating far-field gain based on the magnitude of the power transmission in a Fresnel region is presented, which can be applied to the phaseless near-field measurement. Due to the short range inside an anechoic chamber, the probe antenna is often placed in the Fresnel region of the antenna under test (AUT). It is well-known that far-field gain of an antenna gradually reduces when one antenna moves to the other one placed in a proximity distance. This fact can be advantageously applied to estimate the far-field gain in a far-field region. The proposed method offers rapid estimation of the far-field gain based on the simple input knowledge such as the probe antenna gain and the magnitude of the power transmission and the separation distance between AUT and probe antenna. The proposed method can be applicable to a wide range of microwave antennas. This feature makes it possible to offer preliminary measurement results and reference parameters of the measurement for the various types of microwave antennas.

**Index Terms** — Fresnel region, gain reduction effect, phaseless near-field measurement.

## I. INTRODUCTION

With the emergence of sophisticated radar and telecommunication infrastructures, an estimation of the maximum gain of antenna is an important consideration in order to establish the performance of the system. The far-field measurement has been widely used due to the merits of directly measuring the far-field pattern of the AUT. However, the far-field measurement suffers from an electrically large test range and geometrical intricacy especially for compact antenna test range [1-2]. For the near-field measurement, the probe antenna is situated in the near-field region of AUT, which allows one to employ a smaller test range. Meanwhile, the near-field measurement utilizes the Fourier transform of complex

near-field data to reconstruct the far-field pattern of the AUT [3]. A highly precise hardware is required to directly measure an exact phase information. As an alternative method, the phaseless near-field measurement enables to recover the phase information based on the amplitude measurement [4-6]. The phaseless measurement has been developed to offer an accurate and practical method for antenna measurement and diagnostic means [4-6]. The phase retrieval process has been studied through diverse algorithms with an effort to reduce an error, compared to the direct measurement [4-6]. Recently, reduced number of amplitude measurements with an iterative Fourier procedure has been introduced to recover the far-field pattern for antenna measurement [6].

For the case of predicting the maximum far-field gain, the post-processing of measured data can be further reduced, which does not require an extra step of estimating phase information [7-11]. While there has been restriction on the types of apertures [7-9], the formula in [10, 12] is flexible in terms of not being subject to the types of antenna and operating frequencies. Based on the formula in [10], on-axis far-field gain has been estimated through using the magnitude of the power transmission in the Fresnel region [11], however, complete and practical expression of the far-field gain of AUT has not been presented.

In this paper, an effective method of acquiring the far-field gain based on the antenna coupling collected during the near-field measurement is presented. The proposed method requires the minimal input information such as the magnitude of the power transmission at one distance between AUT and probe antenna as depicted in Fig. 1. The proposed expression of the far-field gain is advantageous with respect to the general applicability to the measurement of diverse antenna applications. This feature significantly simplifies the post-processing of the measured data by estimating the effect of gain reduction

which is simply deduced from one location of the measurement. The validity of the proposed method is evaluated through representative examples of reflector and horn antennas.

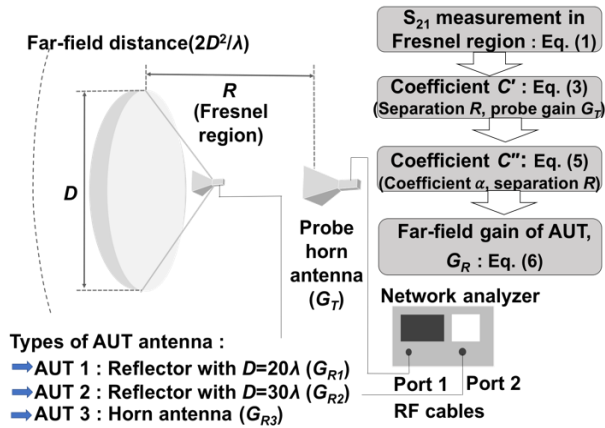


Fig. 1. Overview of this research activities of far-field estimation using the coupling level measured in Fresnel region.

## II. DERIVATION OF FAR-FIELD GAIN USING POWER TRANSMISSION IN FRESNEL REGION

The measurement setup of interest is shown in Fig. 1. The probe horn antenna and AUT are used as transmitting and receiving antenna, respectively. The AUT is situated in the far-field region of the probe horn while the probe horn is positioned within the Fresnel region of the AUT. The power transmission  $\eta$  between a transmitting power  $P_T$  and a receiving power  $P_R$  is presented in [10], which is valid in both Fresnel and far-field region

$$h = \frac{P_R}{P_T} = \left( \frac{l}{4\rho R} \right)^2 G_T g_T G_R g_R, \quad (1)$$

where  $G_T$  and  $G_R$  are on-axis far-field gain of transmitting probe antenna and receiving AUT, respectively, and  $R$  is the distance from the probe to the AUT.  $\gamma_T$  and  $\gamma_R$  are the gain reduction factors of the transmitting antenna and of the receiving antenna, respectively. For the antenna measurement, the AUT is positioned in the far-field region of the probe antenna, therefore,  $\gamma_T$  is set as one. Meanwhile,  $\gamma_R$  is a variable, which reduces from one as the separation distance  $R$  becomes smaller. The gain reduction factor of receiving antenna  $\gamma_R$  can be expressed as the normalized form of separation distance of the receiving antenna  $\Delta_R$ ,

$$g_T = 1, \quad g_R = 1 - aD_R^{-2}, \quad (2)$$

where  $\Delta_R$  can be defined as  $R/(2\lambda G_R/\pi^2)$ . The separation distance normalized with the far-field edge distance of

$2D^2/\lambda$  has been widely used, however, normalizing the separation distance with the far-field edge distance produces the varied coefficient  $\alpha$  according to different types of antennas. On the other hand, with normalizing the separation distance in terms of  $2\lambda G_R/\pi^2$ , a constant coefficient  $\alpha$  of 0.06 can be achieved, which is valid for a wide range of microwave antennas [10].

Based on the magnitude of the power transmission at the separation distance  $R$ , (1) can be expressed as function of far-field gain of AUT,  $G_R$ . Dividing (1) with the far-field gain of the probe  $G_T$  and re-organizing (1) in terms of  $G_R$  and  $\gamma_R$  yields:

$$C' = G_R g_R, \quad (3)$$

where the constant  $C'$  is defined as  $\frac{\eta}{G_T} \left( \frac{\lambda}{4\pi R} \right)^{-2}$ .

The constant  $C'$  can be obtained based on the power transmission  $\eta$  between AUT and probe antenna, which can be obtained from simulation or measurement. Substituting  $\gamma_R$  presented in the formula (2) into the formula (3) produces:

$$C' = G_R \left[ 1 - a \left( \frac{R}{2\lambda G_R / \pi^2} \right)^{-2} \right]. \quad (4)$$

Note that the formula (4) is valid when the far-field gain of AUT,  $G_R$  is higher than 10 dB as presented in [10]. Expanding the applicability of the formula to include the electrically small antenna has been discussed in [10]. The gain reduction factor of the small antenna has been derived by simply adjusting the far-field gain in the normalized form of the separation distance. Either simply changing  $G_R$  into  $2G_R$  or providing a smooth transition from  $G_R$  to  $2G_R$  as presented in (4) will enhance the accuracy of the formula if  $G_R$  is lower than 10 dB (i.e. dipole antenna and waveguide). Based on the normalized form of separation distance, the formula (4) can be written with respect to the far-field gain of AUT,  $G_R$ , and a cubic equation can be expressed in terms of the far-field gain  $G_R$  as following

$$C'' G_R^3 - G_R + C' = 0, \quad (5)$$

where the constant  $C''$  can be written as  $\alpha \left( \frac{R}{2\lambda/\pi^2} \right)^{-2}$ .

The equation (5) provides a meaningful physical interpretation of the far-field gain  $G_R$  as the separation distance  $R$  is varied. The equation (5) produces  $G_R = C'$  in the limit of  $R \rightarrow \infty$ , which implies that the far-field gain  $G_R$  can be derived from the standard Friis formula. Meanwhile, in the limit of  $R \rightarrow 0$ , the equation (5) yields  $G_R = 0$ , which indicates that the far-field gain  $G_R$  decreases to zero in the proximity distance. In the following section, there will be a discussion about the rapid decrease of far-field gain  $G_R$  in the Fresnel region. The analytic solutions to the cubic equation are presented in [13], which can be used to derive the far-field gain of AUT  $G_R$ . If a

discriminant,  $D$  is smaller than zero where  $D$  is defined as  $D = \sqrt{(C'/(2C''))^2 - (1/(3C''))^3}$ , the cubic equation has one real root and two complex conjugates. Since  $D$  is smaller than zero, the far-field gain  $G_R$  can be written as presented in [13],

$$G_R = A \times \sqrt[3]{-\frac{C'}{2C''} + \sqrt{\left(\frac{C'}{2C''}\right)^2 - \left(\frac{1}{3C''}\right)^3}} + B \times \sqrt[3]{-\frac{C'}{2C''} - \sqrt{\left(\frac{C'}{2C''}\right)^2 - \left(\frac{1}{3C''}\right)^3}}, \quad (6)$$

where  $A = -0.5+0.866j$  and  $B = -0.5-0.866j$ . Among the three solutions, one solution in terms of  $A = -0.5+0.866j$  and  $B = -0.5-0.866j$  is selected since it shows a stable far-field gain at the distance of the Fresnel region. The mathematical expression is chosen to acquire the far-field gain of AUT, based on the magnitude of the power transmission in the Fresnel and the far-field distance between probe and AUT. In next Section, the formula (6) is validated through examples of different types of microwave antennas.

### III. EVALUATION OF THE PROPOSED FORMULA

In this Section, the far-field gain is derived using the formula (6) based on the power transmission obtained using FEKO simulation or measurement. The results obtained using (6) are compared to the far-field gain directly measured in anechoic chamber or simulated one acquired using FEKO. Two reflector antennas both operating at 12.7 GHz and horn antenna operating at 10 GHz are chosen to examine the validity of the proposed equation. These antennas are varied in terms of far-field gain at microwave bands. In addition, an effective range of the equation within the Fresnel region is presented in terms of the different normalized distances  $\Delta$ .

#### A. Representative antennas used in the evaluation

The validity of the proposed equation is evaluated employing three types of antennas: a horn antenna and two reflector antennas of a diameter of  $20\lambda$  and  $30\lambda$ . Figures 2 (a) and (b) depicts a configuration of the two  $20\lambda$  and  $30\lambda$  reflector antennas. The  $F/D$  ratio of 0.7 and a 19 dB taper are applied to the both reflector antennas, therefore, the focal length for  $20\lambda$  and  $30\lambda$  reflectors are set as  $14\lambda$  and  $21\lambda$ , respectively. The optimal diameter of the reflector antennas is selected considering the physical length of the test range at 12.7GHz. For the applications operating at higher frequency, the proposed method will provide a degree of freedom to increase the electrical size of the antenna. The dimension of the horn antenna used in the evaluation is depicted in Fig. 2 (c).

Figure 2 (d) shows the simulation setup to obtain the power transmission between AUT and probe antenna which is placed in the near-field region of AUT. A probe antenna for the two reflector antennas and the horn antenna are identical to a standard gain horn antenna with a maximum far-field gain of 15.5 dB at 12.7 GHz and a WR-75 waveguide with 6.3 dB at 10 GHz, respectively. It is worth noting that both probe antennas are all situated at the far-field region of three types of AUT. The radiation patterns of the reflector type of AUTs are obtained using a full-wave simulation tool, FEKO while the radiation pattern of the horn antenna is measured inside an anechoic far-field chamber.

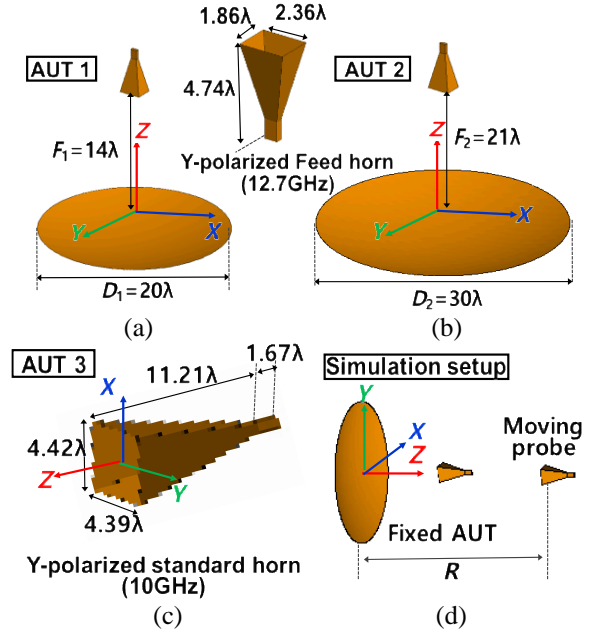
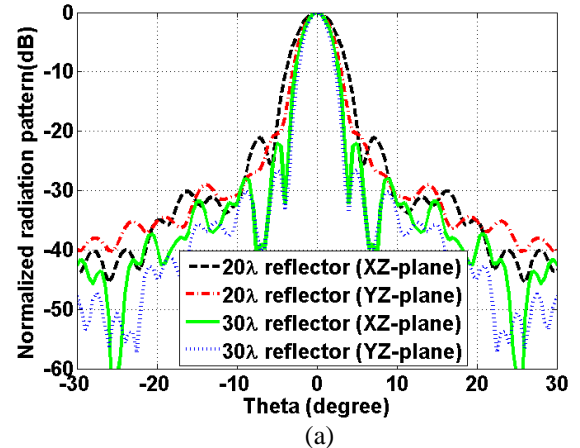


Fig. 2. Configuration of prime focused reflector antenna of: (a) a diameter of  $20\lambda$ , (b) a diameter of  $30\lambda$ , (c) configuration of a standard gain horn antenna, and (d) the setup of the FEKO simulation.



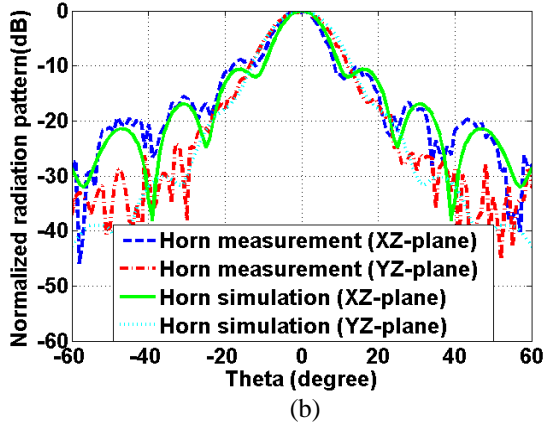


Fig. 3. Normalized radiation patterns of representative antennas: (a) the simulated one of the two reflector antennas, and (b) the measured and simulated one of the horn antenna.

As shown in Fig. 3, the radiation patterns of  $20\lambda$  and  $30\lambda$  reflector antennas are obtained at 12.7 GHz using full-wave simulation, FEKO and maximum gains of two reflector antennas are simulated as 32.8 dB and 35.7 dB, respectively. The radiation pattern of horn antenna is measured at 10 GHz, which shows a good agreement with the radiation pattern obtained using FEKO. The far-field gain obtained from simulation and measurement are 22.8 dB and 22.5 dB, respectively.

### B. Power transmissions and gain reduction factors

The power transmission formula presented in [10] is revisited. Figure 4 shows a comparison of the power transmission in addition to the associated gain reduction factors as separation distances  $R$  is changed. Note that the three representative antennas discussed in previous section are used in this evaluation. The modified Friis formula [10] provides an enhancement of around 2-3 dB in the Fresnel region, compared to the classic Friis formula. The computed result agrees well with the power transmission obtained using FEKO within 0.5 dB deviation except for the failure of the formula in a close distance of the Fresnel region. The power transmission level in Fig. 4 (b) seems to be lower than the one in Fig. 4 (a). However, actually, the power transmission of the Fig. 4 (b) is 2.9dB higher than the one of Fig. 4 (a), which is identical to the difference of the far-field gains between  $20\lambda$  and  $30\lambda$  reflector antennas. Note that this work is different from the previous work [10] in terms of the presence of the corresponding gain reduction factor along with the power transmission. It is observed that the gain reduction factor varies from one to zero when the separation distance  $R$  reduces. The gain reduction factor

agrees well with the enhancement in terms of the power transmission, compared to the classic Friis formula.

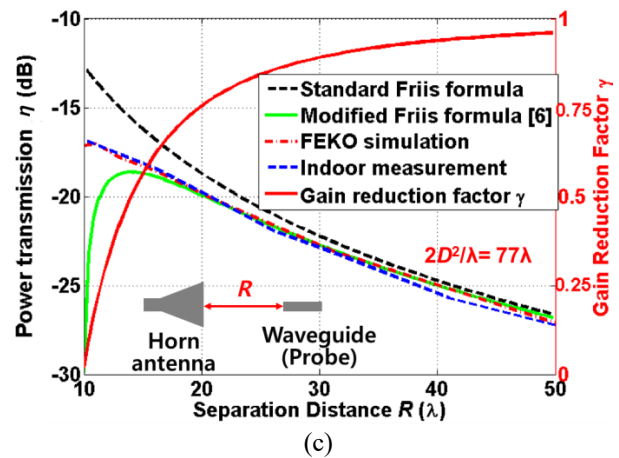
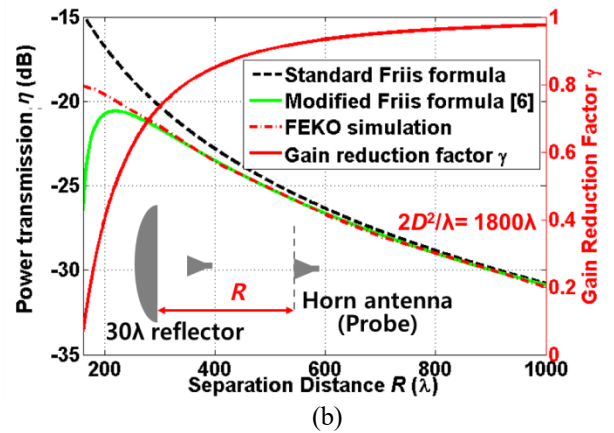
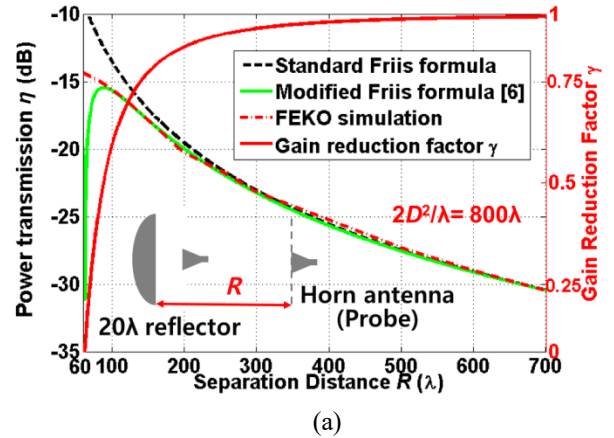


Fig. 4. A comparison of the standard Friis formula, modified Friis formula, FEKO simulation (measurement) and gain reduction factor  $\gamma$ : (a)  $20\lambda$  reflector antenna, (b)  $30\lambda$  reflector antenna, and (c) 10 GHz horn antenna.

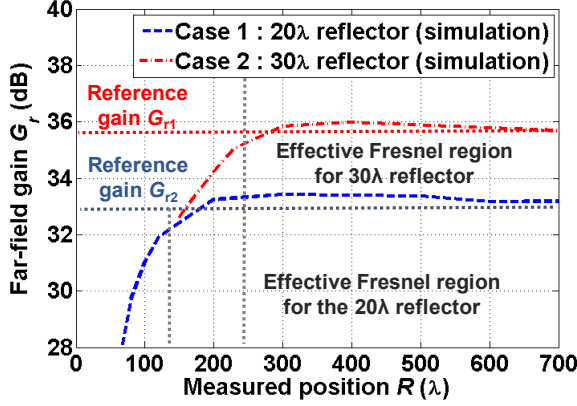


Fig. 5. Computed far-field gain  $G_r$  for the two reflector antennas using the proposed formula based on the simulated power transmission  $\eta$  using FEKO.

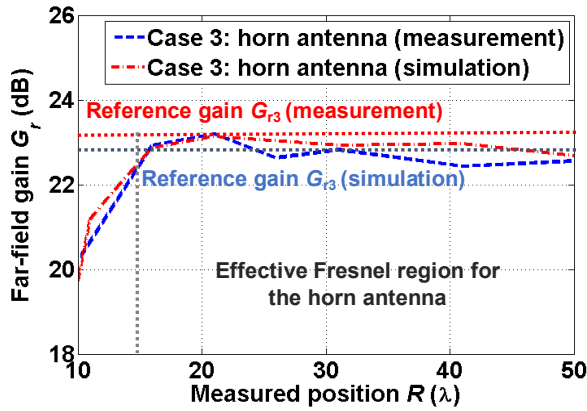


Fig. 6. Computed far-field gain  $G_r$  for the horn antenna based on the simulated and measured power transmission  $\eta$ .

### C. Derivation of far-field gains from near-field measurement

Based on the power transmissions  $\eta$  acquired at the separation distance  $R$ , the formula (6) is used to calculate the far-field gain of AUT. The overall procedure to obtain the far-field gain of AUT is shown in Fig. 1. The power transmission between AUT and probe antenna can be obtained through either a simulation or a measurement at a separation distance in the Fresnel region. Different types of AUT is fixed while the probe antenna is moved along the  $z$  axis by varying a separation distance  $R$  between them. Based on the power transmission  $\eta$ , the gain of probe antenna, and separation distance  $R$ , the coefficient  $C'$  can be calculated. Next step is the calculation of the coefficient  $C''$  that consists of the coefficient  $\alpha$  of 0.06 and separation distance  $R$ . Finally, the far-field gain of the AUT presented in (6) can be calculated based on the coefficient  $C'$  and  $C''$ . In the

previous study in [10], the gain reduction factor is used to correct the Friis formula in the Fresnel region. In this work, the correction factor embedded in the formula (6) is conversely applied to compensate for the effect of the reduced gain in Fresnel region and ultimately achieve the unvarying far-field gain in terms of the measured position  $R$ . The validity of the formula (6) is verified comparing it to the reference far-field gain obtained using a simulation or a measurement. Figure 5 depicts a comparison of the calculated far-field gain  $G_R$  for 20  $\lambda$  and 30  $\lambda$  reflector based on the power transmission obtained using full-wave simulation FEKO. Figure 5 depicts the far-field gain  $G_R$  obtained using (6), which is consistent around the simulated far-field gains of 32.8 dB and 35.7 dB for the 20  $\lambda$  and 30  $\lambda$  reflector antennas, respectively. The stable far-field gain can be obtained even if the probe antenna is placed in the Fresnel region of the AUT. The deviation of the formula (6) in terms of the directly simulated far-field gain is less than 0.5 dB within the effective region of the formula, which can be converted into the percentage error less than 12%. It is reported in [10] that the power transmission is rapidly decreased at a close distance of Fresnel region, which is a failure due to the inclusion of a quadratic form of  $\gamma_R$ . The inherent failure of the formula affects the reduction of the far-field gain  $G_R$  at a close proximity. The far-field gain  $G_R$  of the X-band horn antenna is evaluated based on the power transmission obtained using the both FEKO and measurement. Figure 5 depicts a comparison of the two far-field gain  $G_R$  where a good agreement between simulated and measured far-field gain is observed. The difference between two results is less than 0.7 dB, which can be converted into the percentage error less than 17.5%.

### D. Effective range of the proposed formula

As discussed previously, the accuracy of the formula is deteriorated in a closer separation distance in the Fresnel region. The minimum separation distances are measured at the point that the curves of far-field gain deviates from the reference data obtained using the full-wave simulation, FEKO or indoor measurement. Note that the allowance of the deviation is set as 0.5 dB. The minimum separation distance is approximately measured as 14  $\lambda$  for the horn antenna, 120  $\lambda$  for the 20  $\lambda$  reflector and 230  $\lambda$  for the 30  $\lambda$  reflector. It is observed that the closer minimum separation distance can be obtained for the antennas with a smaller aperture, which is presented in Table 1. It is desirable to present the effective range of the formula depending on the normalized distance of  $2D^2/\lambda$  or  $2\lambda G/\pi^2$ . First, the separation distance  $R$  can be normalized in terms of  $2D^2/\lambda$ , which is relevant to the aperture size of the antenna. Second, the separation distance  $R$  can be normalized in terms of  $2\lambda G/\pi^2$ , which is based on the far-field gain of the antenna. The distances calculated from the normalization of  $2D^2/\lambda$  are approximately 77.4  $\lambda$ , 800



$\lambda$  and  $1800 \lambda$  for the horn antenna,  $10 \lambda$  and  $20 \lambda$  reflector antenna, respectively. The distances calculated from the normalization of  $2\lambda G/\pi^2$  are  $36 \lambda$ ,  $386 \lambda$ , and  $753 \lambda$  for the horn antenna,  $10 \lambda$  and  $20 \lambda$  reflector antenna, respectively. The nearest distances in terms of different normalization,  $2D^2/\lambda$  and  $2\lambda G/\pi^2$  and aperture areas for the representative antennas used in the evaluation are presented in Table 1. The minimum separation distances using the different normalizations varies from 0.128 to 0.181 in terms of  $2D^2/\lambda$  and from 0.305 to 0.389 in terms of  $2\lambda G/\pi^2$ . It is shown that the minimum distances tend to slightly increase as the size of the aperture is decreased. This is attributed to the fact that the accuracy of the formula becomes worse as the far-field gains of the antennas reduce to the lower bound of the effective far-field gain which is around 10 dB.

Table 1: Effective minimum separation distance and physical aperture areas

	$2D^2/\lambda$	$2\lambda G/\pi^2$	Physical Aperture Areas
Horn antenna	$0.181 \times (2D^2/\lambda)$	$0.389 \times (2\lambda G/\pi^2)$	$19.4 \lambda^2$ (0.0174 m <sup>2</sup> )
Reflector 1	$0.150 \times (2D^2/\lambda)$	$0.311 \times (2\lambda G/\pi^2)$	$400\pi \lambda^2$ (0.7 m <sup>2</sup> )
Reflector 2	$0.128 \times (2D^2/\lambda)$	$0.305 \times (2\lambda G/\pi^2)$	$900\pi \lambda^2$ (1.578 m <sup>2</sup> )

#### IV. CONCLUSION

In this paper, an effective method of estimating the maximum far-field gain based on magnitude of the power transmission is presented. The proposed expression of the far-field gain is advantageous since it offers convenience of the calculation merely using the magnitude of the power transmission at one point of separation distance. The validity of the proposed method is evaluated through representative examples such as one horn antenna and two reflector antennas. The calculated results show an excellent agreement with the measured results in an anechoic chamber within part of Fresnel region. The effective test range of the formula is presented in terms of normalizing distances  $2D^2/\lambda$  and  $2\lambda G/\pi^2$ , and it is demonstrated that the range is adequate for the near-field measurement.

#### ACKNOWLEDGMENT

The research work of the two authors, Sun-Gyu Lee and Jeong-Hae Lee was supported by Basic Science Research Program through the National Research Foundation of Korea (NRF) funded by the Ministry of Education (No. 2015R1A6A1A03031833).

#### REFERENCES

- [1] C. A. Balanis, *Antenna Theory: Analysis and Design*. 3rd ed., Wiley Interscience, 2005.
- [2] O. Borries, P. Meincke, E. Jørgensen, and, C. H. Schmidt, "Design and validation of compact antenna test ranges using computational EM," *Proc. AMTA 37th Annual Meeting*, pp. 40-45, Oct. 2015.
- [3] A. D. Yaghjian, "An overview of near-field antenna measurements," *IEEE Trans. Antennas Propag.*, vol. 34, pp. 30-45, Jan. 1986.
- [4] R. G. Yaccarino and Y. Rahmat-Samii, "Phaseless bi-polar planar near-field measurements and diagnostics of array antennas," *IEEE Trans. Antennas Propag.*, vol. 47, no. 3, pp. 574-583, Mar. 1999.
- [5] S. F. Razavi and Y. Rahmat-Samii, "A new look at phaseless planar near-field measurements: limitations, simulations, measurements, and a hybrid solution," *IEEE Trans. Antennas Propag. Magazine*, vol. 49, no. 2, pp. 170-178, Apr. 2007.
- [6] S. F. Razavi and Y. Rahmat-Samii, "On the uniqueness of planar near-field phaseless antenna measurements based on two amplitude-only measurements," *2008 IEEE Int. Symp. on Antennas and Propag.*, July 5-11, 2008.
- [7] J. R. Pace, "Asymptotic formulas for coupling between two antennas in the Fresnel region," *IEEE Trans. Antennas Propag.*, AP-17, no. 3, pp. 285-291, 1969.
- [8] T. S. Chu, "An approximate generalization of the Friis transmission formula," *Proc. IEEE*, pp. 296-297, Mar. 1965.
- [9] Y. Kim, S. Boo, G. Kim, N. Kim, and B. Lee, "Wireless power transfer efficiency formula applicable in near and far fields," *Journal of Electromagn. Eng. Sci.*, vol. 19, no. 4, pp. 239-244, Oct. 2019.
- [10] I. Kim, S. Xu, and Y. Rahmat-Samii, "Generalised correction to the Friis formula: Quick determination of the coupling in the Fresnel region," *IET Microw. Antennas and Propag.*, vol. 7, no. 13, pp. 1092-1101, Oct. 2013.
- [11] I. Kim and S. Lee, "Estimation of the maximum directivity of the antennas using the mutual coupling between two antennas," *2018 Int. Symp. on Antennas and Propag.(ISAP)*, Oct. 23-26. 2018.
- [12] I. Kim, C. Lee and J. Lee, "On computing the mutual coupling between two antennas," *IEEE Trans. Antennas Propag.*, doi:10.1109/TAP.2020.2989899.
- [13] M. R. Spiegel, *Mathematical Handbook of Formulas and Tables*, 5th ed., New Jersey, McGraw-Hill Education, 2017.



**Ilkyu Kim** received his B.S. degree in Electrical Engineering from Hongik University, Seoul, South Korea in 2003 and the M.S. degree in Electrical Engineering from University of Southern California, Los Angeles, CA in 2006 and Ph.D. degrees in Electrical Engineering from University of California at Los Angeles in 2012. He was with Samsung Advanced Institute of Technology from 2006 to 2008. After gaining his Ph.D. degree, he joined in Defense Agency for Technology Quality, Daejeon, South Korea, where he is currently working as a senior research engineer in the area of radar and space applications. His research interests include but not limited to computation of electromagnetic mutual coupling, antenna measurement, and antenna design for space and radar applications.



**Sun-Gyu Lee** received B.S. and M.S. degrees in Electronic and Electrical Engineering from Hongik University in Seoul, Republic of Korea in 2016 and 2018, respectively. He is currently working toward a Ph.D. degree at the same institution. His research interests include phased array antennas and metasurfaces.



**Jeong-Hae Lee** received B.S. and M.S. degrees in Electrical Engineering from Seoul National University in Korea in 1985 and 1988, respectively, and a Ph.D. degree in Electrical Engineering from the University of California, LA in 1996. From 1993 to 1996, he was a Visiting Scientist of General Atomics in San Diego, CA, where his major research initiatives were developing a millimeter-wave diagnostic system and studying plasma wave propagation. Since 1996, he has been working at Hongik University in Seoul, Korea as a Professor in the Department of Electronic and Electrical Engineering. He has more than 100 papers published in journals and 60 patents. He was a president of the Korea Institute of Electromagnetic Engineering and Science in 2019. He is currently a Director of the Metamaterial Electronic Device Center. His current research interests include metamaterial radio frequency devices and wireless power transfer.